Comparative Molecular Field Analysis of Dopamine D4 Receptor Antagonists Including 3-[4-(4-Chlorophenyl)piperazin-1-ylmethyl]pyrazolo[1,5-*a*]pyridine (FAUC 113), 3-[4-(4-Chlorophenyl)piperazin-1-ylmethyl]-1*H*-pyrrolo-[2,3-*b*]pyridine (L-745,870), and Clozapine

Harald Lanig, Wolfgang Utz, and Peter Gmeiner*

Department of Medicinal Chemistry, Emil Fischer Center, Friedrich-Alexander University, Schuhstrasse 19, D-91052 Erlangen, Germany

Received August 7, 2000

A CoMFA study was undertaken to elucidate the correlation of biological activity and structural parameters of 25 dopamine D4 antagonists. A special point of interest is that we have included the atypical D4 antagonist clozapine as a structural template for all other compounds. After comparing potential protonation sites at semiempirical (AM1) and ab initio (6-31G(d)) levels of theory, possible conformations of the lead compound 3-[4-(4-chlorophenyl)piperazin-1-ylmethyl]pyrazolo[1,5-*a*]pyridine (FAUC 113) were investigated by systematic semiempirical conformational analysis. The final conformation of FAUC 113, which was used as a template for the other compounds in the dataset, was chosen by clustering and rigid body alignment of all conformations to clozapine. The CoMFA applied on the final alignment resulted in a q^2_{cv} of 0.739. To elucidate the influence of the absolute orientation of the molecules within the grid space, the entire dataset was systematically rotated (1296 steps) within the lattice. The Gaussian-shaped distribution of the q^2_{cv} values spanned the range of 0.699−0.794 and therefore supports the significance of the analysis.

Introduction

The application of molecular cloning techniques led to the characterization of five different dopamine receptors, which can be classified into two classes, D1-like (D1 and D5) and D2-like (D2, D3, and D4), all belonging to the superfamily of G protein coupled receptors.[1−3] The atypical antipsychotic agent clozapine shows preferential binding to the D4 subtype.[4] This minimizes extrapyramidal side effects and movement disorders as it does not affect the dopaminergic activities of other receptor subtypes. Therefore, the development of selective D4 receptor antagonists has become an active field of research, and many intensive structure−activity relationship (SAR) studies have been performed.[5−20]

Recent SAR studies of our group have given insight into the molecular properties causing D4 receptor affinity and selectivity.[21−24] In this work, the main objective was to evaluate the molecular properties which determine the binding to the D4 receptor. This was done by applying the comparative molecular field analysis (CoMFA) technique[25] to a set of 25 D4 receptor antagonists. Special emphasis was taken on the fact that clozapine, which does not match the common structural pattern of the other ligands used in this study, was included in the molecular field analysis at the very beginning. Recent QSAR studies on the dopamine receptor subtypes D1, D2, and D3 have been published.[26−29]

Methods

Compounds and Measurement of Drug Affinities. While compounds **1**−**23** and **26**−**29** have been synthesized in our laboratory, L-745,870 (**24**) and clozapine (**25**) were obtained from Sigma-Aldrich, Taufkirchen, Germany. Receptor binding profiles of all compounds were determined by measuring their ability to displace [^{3}H]spiperone[23] from the cloned human D4.4 receptor subtype, expressed in CHO-K1 cells.[30] Table 1 gives an overview of all compounds used in this study. Except for compounds **4** and **23**, which have been synthesized according to the methodology described in ref 31, all ligands have been previously published.[21−23,31] Compounds **26**−**29** served as a test set for the validation of our model and therefore were not included during the analysis.

Template Selection and Protonation State of the Compounds. To understand specifically the D4 binding (as opposed to D2 binding), we included clozapine in the MFA as the initial template, because of its atypical behavior exhibiting an approximately 10-fold selectivity for D4 versus D2 receptors.[32] To use clozapine as a template, it is important that the correct protonation state is used for the alignments. It is assumed in the literature that piperazinyldibenzodiazepines are dibasic compounds and exist as monoprotonated species under physiological conditions. The pK_a value of the distal nitrogen (N_1 in Figure 1) has been reported to be between 7.2 and 7.8, and the pK_a value of the proximal nitrogen N_2, which forms part of the amidine group, is between 2 and 5.[33] This means that under physiological conditions, N_1 should be protonated to an extent of 40−70%, while N_2 should be unprotonated. However, another group was unable to titrate the proximal nitrogen atom of the piperazine ring within their series of compounds. For clozapine, a pK_a value of 7.25 for nitrogen N_1 has been observed.[34]

Due to the lack of clear experimental evidence which nitrogen is protonated first and the fact that four nitrogens could be protonated in principle but only one or two protonation steps have been observed, we calculated the enthalpy ΔH_f^{298} for the reaction Clz + H^+ → ClzH^+ for all nitrogens using semiempirical (AM1)[35] and ab initio (6-31G(d))[36] levels of theory. To account for solvent effects, a self-consistent reaction field (SCRF) based on the Onsager model was applied. Furthermore, the gas-phase geometries were reoptimized

* To whom correspondence should be addressed. Tel: ++49-9131-85-29383. Fax: ++49-9131-85-22585. E-mail: gmeiner@pharmazie.uni-erlangen.de.

10.1021/jm001055e CCC: $20.00
Published on Web 03/10/2001

Table 1. Piperazine Derivatives Used in This Investigation[a]

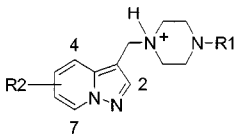

	R1	R2	pK$_i$(D4)
1	p-Cl-Ph	H	8.64
2	Ph	H	7.78
3	p-I-Ph	H	8.52
4	p-F-Ph	H	7.70
5	Me	H	5.14
6	Et	H	4.62
7	p-Cl-Ph	4-Me	7.30
8	p-Cl-Ph	7-I	8.30
9	p-Cl-Ph	7-Me	8.57
10	p-Cl-Ph	7-Ethinyl	8.91
11	Cyclohexyl	H	5.35
12	m-Cl-Ph	H	8.41

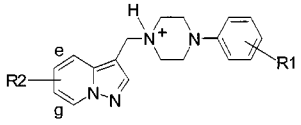

	R1	R2	pK$_i$(D4)
13	p-Cl	Benzo[e]	5.74
14	p-Cl	Benzo[g]	6.85
15	m-Cl	Benzo[e]	6.10
16	m-Cl	Benzo[g]	6.66

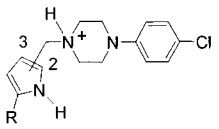

	R	Pyrrole	pK$_i$(D4)
17	H	2	7.58
18	Dicyanovinyl	2	8.02
19	H	3	7.41
20	Dicyanovinyl	3	8.24

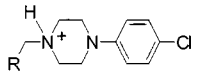

	R	pK$_i$(D4)
21		7.74
22		8.66
23		6.60
24		9.21
25	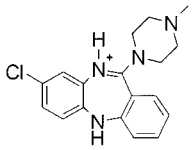	7.80

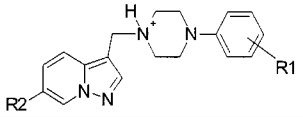

	R1	R2	pK$_i$(D4)
26	p-Ethinyl	H	8.36
27	m,p-Cl	H	8.25
28	m-CF$_3$	H	8.72
29	H	CH_2OH	7.71

[a] All compounds are depicted in their monoprotonated form, which was used throughout all analyses. D4 denotes the negative logarithmic values of the experimentally determined binding affinities to the human D4.4 receptor.

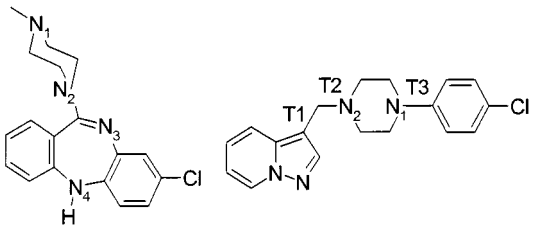

25 1

Figure 1. Possible nitrogen protonation sites of clozapine (**25**, left) and the template compound FAUC 113 (**1**, right), both depicted in their neutral form. In both cases, N_1 is often denoted as the distal and N_2 as the proximal nitrogen. The torsional degrees of freedom scanned by the systematic conformational search of **1** are marked T1, T2, and T3.

using the COSMO[37] approach implemented in VAMP and the especially parametrized AM1-SM2.1 Hamiltonian[38] available within AMSOL.[39] In all cases, zero-point energy corrections were included by frequency calculations on the structures. Table 2 shows the results for the first protonation step. The semiempirical data obtained for the possible monoprotonated isomers clearly indicate that on a thermodynamical basis, this step should occur at the amidinic nitrogen N_3. On the other hand, ab initio SCRF calculations and NMR experiments give evidence for protonation at N_1. All data show that protonation at N_2 is energetically disfavored. Taking into account that solvation phenomena in solution can only be partially transferred to the active site situation, we decided to use the N_3-protonated form of clozapine as a template for all subsequent calculations.

As a representative compound of the dataset, we used the phenylpiperazine derivative FAUC 113 (**1**). On the one hand, it showed an excellent binding affinity to the D4 receptor; on the other hand, it also served as structural basis during the design process of most of the other ligands. Considering the facts already discussed for clozapine, we expect that **1** should also be monoprotonated under physiological conditions. To decide which of the two nitrogens N_1 and N_2 is protonated, we calculated the enthalpies of protonation in the same manner as described above. Using the AM1 Hamiltonian, $\Delta H_f^{298}(N_1)$ amounts to −161.34 kcal/mol and $\Delta H_f^{298}(N_2)$ to −165.43 kcal/mol, which is very close to the experimentally determined enthalpy of protonation for a water molecule (−165.3 ± 1.8 kcal/mol).[40] The preference of N_2 is further supported by the fact that the lone pair of N_1 is in conjugation with the aromatic system of the phenyl ring and therefore is not ideally situated for protonation. For these reasons we used the N_2-protonated isomers of compounds **1**−**24** for all subsequent calculations.

Table 2. Calculated Heats of Protonation for the Reaction Clz + H^+ → ClzH$^+$ at 298 K[a]

site	AM1 (gas/SCRF)	6-31G(d) (gas/SCRF)	AM1 COSMO	AM1 SM2.1
N_1	−160.4/−203.4	−234.2/−252.3	−207.7	−205.2
N_2	−161.7/−194.9	−228.3/−230.0	−197.4	−193.3
N_3	−175.8/−208.5	−244.9/−243.8	−209.6	−207.3

[a] Gas phase and solvent, both kcal/mol. Thermal energy (zero-point) correction was included by frequency calculations on the optimized structures; the translational energy of the proton ($^3/_2RT$ = 0.89 kcal/mol) was also taken into account. In the case of AM1, the heat of formation of the proton is parametrized to 314.91 kcal/mol. The ab initio values are based on the thermal enthalpy-corrected SCF energies. Corrections to the thermal free (Gibbs) energies yielded about 0.2 kcal/mol lower values. Solvation effects were calculated by applying a self-consistent reaction field (SCRF) based on the Onsager model upon the ab initio and semiempirical gas phase geometries. It should be noticed that the Onsager model within Gaussian 94 uses a spherical cavity, while all other implementations apply a van der Waals surface of the molecule. Therefore, the ab initio solvent corrections should be taken with care, especially in the case of N_2 and N_3, which both are located inside the cavity. To account for possible conformational changes caused by solvation, the geometries were reoptimized by either including the COSMO approach or the SM2.1 Hamiltonian parametrized for aqueous solvation.

Molecule Conformations. It is well-known that flexible molecules are by far the most difficult when analyzing ligands to generate a CoMFA model.[41] This critical step of selecting a conformation for each ligand is further complicated by the fact that binding to a protein can occur in different modes or

orientations[42] and that the protein-bound conformation of the ligand is not necessarily the most stable conformation or even a local minimum on the potential energy surface. Due to torsional flexibility within the drug, the receptor is able to optimize the interaction energy in terms of electrostatic, hydrogen bond, and steric contributions. Thus, the minimum-energy conformation of any systematic or random conformational search approach may only partially reflect the real situation.

To obtain information about suitable conformations of clozapine, we first searched the Cambridge Crystallographic Database for corresponding entries. All four clozapine structures available contain the piperazine ring in a chairlike conformation with two equatorial substitutions. We therefore kept the piperazine ring unchanged and focused our search on the rotatable bond connecting the piperazine moiety with the aromatic tricycle. This was done by a systematic rotation about this bond in 20° steps, followed by a semiempirical AM1 geometry optimization of the remaining degrees of freedom. The rotation profile obtained showed two local minima, which can be interconverted by rotating the piperazine ring by almost 180°. The difference in the heat of formation of the two local minima is only 0.16 kcal/mol, indicating only very minor thermodynamic preference. The interconversion barrier calculated for gas-phase conditions is 8.8 kcal/mol, which could in principle be overcome by the binding to the receptor. Due to the fact that the main difference of the two conformations is the orientation of the lone pairs at N_1 and N_2, both orientations were considered during the subsequent alignment process. As already discussed in the previous chapter, all calculations have been performed using the N_3-protonated form of clozapine.

It is of paramount importance to find a conformation for template **1** that ideally fits to clozapine, which shows the lowest flexibility in the dataset, because the geometries of all other molecules and the performance of the CoMFA will depend on it. To obtain suitable geometries for template **1**, we analyzed its conformational space by systematically varying the torsional angles T1, T2, and T3 in 30°, 30°, and 60° steps, respectively (Figure 1). After changing the geometry, the molecule was semiempirically optimized with VAMP's built-in TORQUE function[43] using the AM1 Hamiltonian without any constraints. The maximal number of conformations ($12 \times 12 \times 6 = 864$) is unlikely to be obtained, because different starting geometries may optimize to the same local minimum on the potential energy surface. In total, we obtained 12 different energetically favored conformations for **1** as possible template candidates for the CoMFA. Their ΔH_f values differed by a maximum 2 kcal/mol only, which means that no thermodynamic preference of a single conformation can be ascribed.

One possible way to account for the energetic difference between the global minimum and the active conformation bound to the receptor is to correct the experimental pK_i value according to the following equation:

$$K_i = \frac{[\text{Ligand}_{g,s}][\text{Receptor}_s]}{[\text{Complex}_b]} = \frac{[\text{Ligand}_{g,s}]}{[\text{Ligand}_{b,s}]} \times \frac{[\text{Ligand}_{b,s}][\text{Receptor}_s]}{[\text{Complex}_b]}$$

where g denotes the global minimum conformation, b the bound conformation of the ligand, and s the solvated interaction partner. The fraction on the far right is represented by the CoMFA, because the ligand used is assumed to adopt the bound conformation. Therefore the measured K_i value has to be corrected by the energetic difference of the ligand's bound and global minimum conformations.

In the present study, the energetic differences of the conformers used in the analysis versus their global minima are very small (e.g. 0.13 kcal/mol for **1**). Therefore the conformational correction of K_i can be neglected.

Alignment. All conformations computed for the N_2-protonated **1** were aligned to both N_3-protonated minima of clozapine. In addition to the selection of the appropriate template−conformer pair, this is an essential step to a successful CoMFA. To actually perform an alignment, different techniques exist. Due to the structural differences between clozapine and **1**, an atom-by-atom root-mean-square distance minimization of the aromatic carbons and/or heteroatoms did not seem useful. Therefore we chose the module ASP[44] as implemented in the QSAR package TSAR,[45] which enabled us to perform an alignment by comparison of steric overlap and molecular electrostatic potentials. First, VESPA charges[46] were calculated for clozapine and all the conformations of **1** using the semiempirical program package VAMP. These atom-centered partial charges are obtained by a fit of the electronic wave function to the atomic positions. Compared to other charge schemes such as Coulson or Mulliken, they have the advantage that the anisotropy of the electron distribution around the molecule, especially for aromatic systems, is described in more detail.

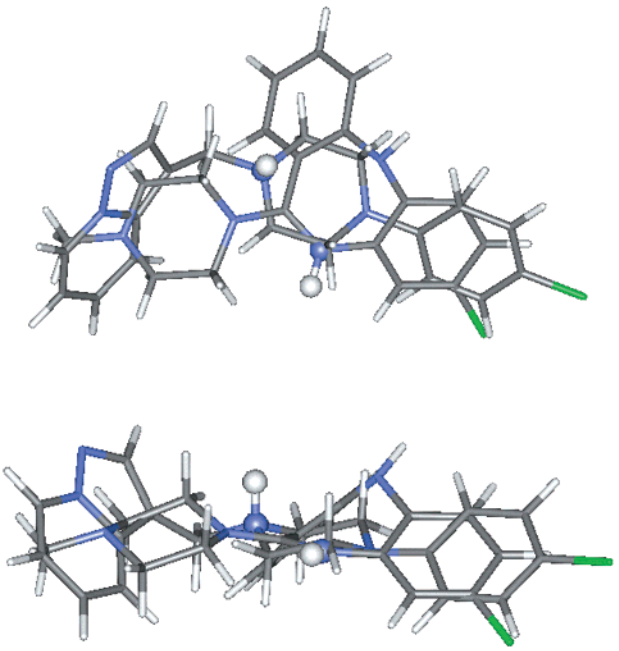

Figure 2. Two different views of the overlay of clozapine with the conformation of FAUC 113 showing the highest combined similarity score after translational and rotational optimization. The protonated nitrogens are represented by balls. Note that there is no direct match of the nitrogens, which are generally considered important pharmacophoric points.

To quantify the relative orientation of two molecules, a combined similarity index based on the Carbo index for electrostatics[47] and a shape similarity index to account for steric differences was evaluated using three Gaussian functions for integration. This combined index was then optimized by performing a full translational and orientational search of the rigid comparison molecule relative to the lead **25** by systematically rotating around the Cartesian *x*-, *y*-, and *z*-axes in 30° steps. For each new orientation, a Simplex algorithm in combination with Simulated Annealing directs the six degrees of freedom to an alignment with optimal similarity.[44] For each of the 12 conformations of **1**, the relative orientation to the two conformations of clozapine was calculated to achieve an optimal similarity index. Out of these orientations, the template conformer was chosen by the highest score combined with visual inspection. This was necessary because some pairs with high alignment scores did not match the chlorine atoms. An overlay of the best fitting pair of molecules in two different views is shown in Figure 2. It should be noted that the algorithm did not only try to fit the nitrogens as close as possible but also includes a steric component by choosing a conformer of **1** which has approximately the same overall shape as clozapine.

Table 3. Summary of the CoMFA Results[a]

orientation validation	original		after systematic search	
	leave-1-out		leave-1-out	
components	7	7	7	7
q^2	0.739	0.996	0.784	0.997
$s_{c/v}$	0.734		0.693	
F		581.7		701.5
fraction (steric/electro)	0.677/ 0.323	0.773/ 0.227	0.677/ 0.323	0.783/ 0.217
grid increment	1 Å	1 Å	1 Å	1 Å

[a] Each analysis started with 10 components. The number of components given in the table showed the lowest standard error of prediction $s_{c/v}$. The last column gives the nonvalidated results for the final orientation of the aligned molecules within the grid lattice.

The conformation of the molecules **2**−**4** and **8**−**10** and their orientation relative to **25** were directly derived from **1**. After performing the necessary changes (e.g. transforming chlorine to fluorine), the bond length was adjusted to standard values as implemented in SYBYL,[48] followed by a geometry relaxation and the calculation of VESPA charges on the final coordinates. The remaining molecules showed larger structural differences when compared to **1**. Here, molecular structure generation was also done starting from **1**, followed by minimizing the geometries to a gradient of 0.1 kcal/(mol Å) using the Tripos force field[49] with Gasteiger−Marsili charges.[50] After minimization, VESPA charges were assigned. Finally, all deduced 23 conformers were re-aligned on **1** with ASP to get a consistent dataset.

CoMFA. The descriptive steric and electrostatic components of the intermolecular interaction field were calculated as implemented in SYBYL using Coulomb and Lennard−Jones potentials, respectively. The analysis was performed using a sp^3 carbon probe (C.3, charge +1.0) positioned at the lattice points (1 Å increment) of a regular grid. It was dimensioned to ensure that the distance of all atoms to the grid borders was at least 4 Å. Column filtering was set to 2.0 kcal/mol, steric and electrostatic cutoffs to 30 kcal/mol with smooth transition. The obtained data were regressed by a partial-least-squares analysis[51] to the target property pK_i (−log K_i). To check the statistical significance of the models, cross-validations by the "leave-one-out" method were performed. The optimal number of components was determined by the smallest standard error of prediction $s_{c/v}$. This value, which does not necessarily correspond to the highest q^2_{cv}, was used to derive the final QSAR model. The statistical data are summarized in Table 3, and the plots of the predicted versus the experimental binding affinities are shown in Figure 3.

To account for possible problems of the analysis arising with the absolute orientation of the molecules within the grid space,[52] it is useful to translate and/or rotate the entire dataset within the lattice. This can be done manually by using the STATIC TRANSLATE or STATIC ROTATE commands in SYBYL. Wang et al.[53] automated this task by providing a SPL script which systematically varies the position of all molecules in the dataset without changing their relative orientation. After each of 1296 reorientation steps, the PLS analysis was repeated. This procedure gives detailed information about the rotational dependence of the CoMFA.

Results

CoMFA. The initial PLS analysis of our aligned dataset yielded a cross-validated q^2 of 0.757 with $s_{c/v}$ = 0.781 using 10 components. After repeating the analysis with 7 components at minimal $s_{c/v}$ = 0.734, the q^2_{cv} decreased to 0.739.

Böhm et al. attribute the dependence of q^2_{cv} on the grid spacing and the absolute position of the aligned molecules within the lattice to the shape and steepness of the hyperbolic Lennard−Jones and Coulomb potentials used during the analysis.[54] They stated that in the

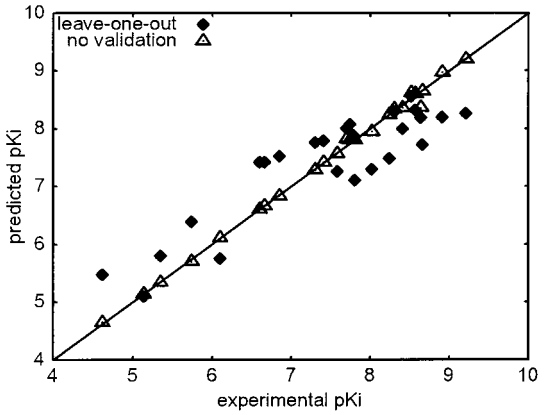

Figure 3. Predicted versus experimental binding affinities (pK_i) for the 24 D4 antagonists and clozapine included in the dataset. Shown is the data for the best model after systematic orientation of the aligned molecules within the lattice. The q^2_{cv} value is 0.784, in the case of the nonvalidated prediction r^2 = 0.997, standard error of estimate s = 0.087.

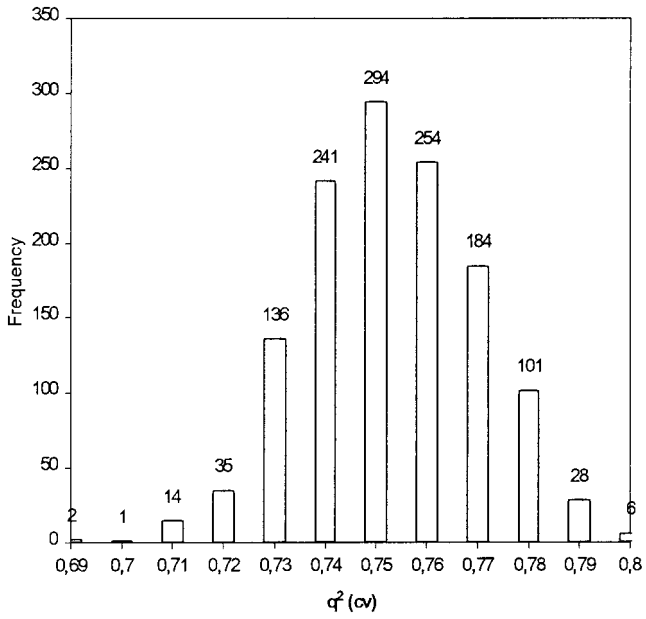

Figure 4. Histogram showing the distribution of the q^2_{cv} values after leave-one-out cross-validation calculated by systematic variation of the orientation of the aligned molecules within the lattice. The numbers on top of the bars indicate how many data point values lie within the respective q^2 range.

case of a 2 Å lattice, important contributions to the correlation analysis could be lost due to the required arbitrary cutoff values. Despite the fact that changing from a 2 to 1 Å lattice spacing results in an increase in computing time by a factor of 8, we performed all analyses also using the smaller increment. To quantify the orientational dependence of q^2_{cv}, we applied a procedure published by Wang et al. which systematically rotates the aligned dataset in space, followed by a PLS analysis after every reorientation. Figure 4 shows the Gaussian-shaped distribution of the obtained q^2 values (1 Å lattice). The range of the values (0.688−0.794) is quite narrow. The highest q^2_{cv} (0.794) was found for 9 components with $s_{c/v}$ = 0.720. For 7 components, the standard deviation $s_{c/v}$ was minimal (0.693), yielding a final q^2_{cv} = 0.784. Modification of the CoMFA parameters, such as changing cutoff values for steric/electrostatic energies, including hydrophobicity data

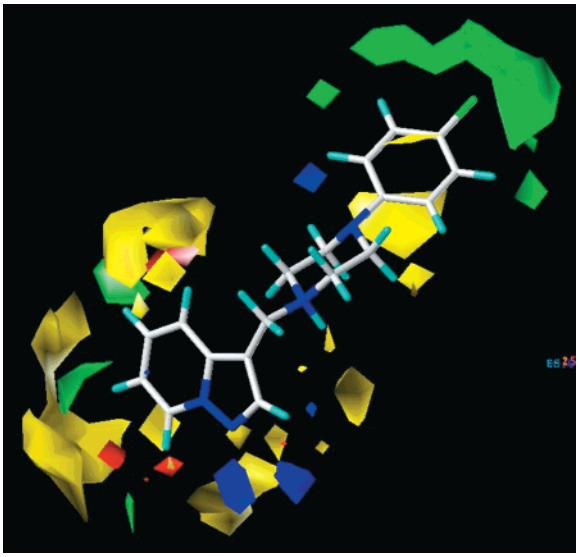

Figure 5. Graphical representation of the final CoMFA field. The color coding of the areas is as follows: green = steric favored, yellow = steric disfavored, blue = positive electrostatic favored, red = positive electrostatic disfavored.

from CoMSIA,[55] varying the field types (indicator, parabolic, H-bond), dipole moments, molecular weight, and refractivity, did not give any improvement of the model.

Comparing the optimal value before (0.739) and after the systematic change in orientation of the molecules (0.784), we obtained some improvement in the statistics (0.045), but the orientational dependence of the statistics is not as large as expected. For our dataset and alignment, the rotational variance of the CoMFA is negligible when applying a grid spacing of 1 Å.

When rotating the aligned compounds within a 2 Å lattice, the q^2_{cv} deviation is considerably larger ($\Delta q^2_{cv} = 0.413$). The orientation with the best statistics gave a $q^2_{cv} = 0.803$ using 5 components, which is slightly better than the result of the 1.0 Å case. Nevertheless, we deem the model with the smaller spacing as more stable when adding new compounds to the training set. Therefore we decided to use the small-grid increment for the subsequent analyses.

Graphical Interpretation of the Results. The three-dimensional representation of the CoMFA data as contour plots allows the correlation of experimentally determined affinity data with changes in steric (green/yellow) or electrostatic (blue/red) properties (Figure 5). As a guide, the template compound **1** is shown embedded into the final field as a representative example.

1. Steric Contributions. The part of the antagonists which is made up by *p*-chlorophenyl in most cases is contoured green, indicating that the model favors sterically demanding groups in that area. However, it should be noticed that not all bulky substituents increase the binding affinity compared to the unsubstituted phenyl moiety. The van der Waals radius of chlorine sets a lower limit for a positive effect on the binding affinity (F: 1.36 Å, 7.70; Cl: 1.70 Å, 8.64; I: 2.02 Å, 8.52). In the case of *p*-fluorophenyl (compound **4**) the decrease in activity is large and may be attributed to the smaller steric demand of fluorine compared to chlorine. The different electrostatic properties of **1** and **3** compared to **4** are of minor importance for their activity. Substituting *p*-chlorophenyl by methyl (**5**) or ethyl (**6**) significantly reduces the binding affinity to the D4 receptor.

Table 4. Predictions of pK_i Values of Test Compounds Compared to Experimentally Determined D4 Receptor Affinities

test set	pK_i (exptl)	pK_i (pred)	residual
26	8.36	7.97	0.39
27	8.25	8.70	−0.45
28	8.72	7.88	0.84
29	7.71	7.50	0.21

The yellow surface also located in the *p*-chlorophenyl area indicates a region where steric contributions are disfavored. This is caused by the compounds **5**, **6**, and **11**, in which the *p*-chlorophenyl group is replaced by a methyl, ethyl, or cyclohexyl group, respectively. All three ligands show low binding affinities, especially the ethyl chain and the cyclohexyl ring which are oriented in a sterically unfavorable way. This is represented by the yellow region.

In the pyrazolopyridine area of the molecules, two yellow regions dominate the steric field. In both cases, the binding affinity to the D4 receptor is decreased considerably by fusing a benzene ring to compound **1** in the [*e*] (compound **13**) or [*g*] (compound **14**) position. The same principal behavior can be observed when starting from the *m*-chlorophenyl isomer **12**, leading to compounds **15** and **16**. Adding a methyl group at position 4 of the pyrazolopyridine ring (compound **7**) also results in a loss of binding affinity of more than 1 order of magnitude. In contrast, substituting position 7 of the pyrazolopyridine moiety has a small deactivating (compounds **8** and **9**) or even activating (compound **10**) influence on the receptor binding. The latter effect is discussed in the next section.

2. Electrostatic Contributions. The electrostatic contribution to the overall molecular field is only 28% and therefore more difficult to interpret. Figure 5 shows a blue area in the vicinity of the pyrazolopyridine nitrogen atoms. In this case the field suggests that a positive area within the molecule should enhance the binding affinity. The main reason for this fact is the protonated nitrogen within the pyrrolopyridine unit of compound **24**, which has the best binding affinity of the whole dataset. Negative areas within a ligand should be favorable at position 7 of the pyrazolopyridine ring, as indicated by the corresponding red area. This prediction is supported by the presence of the 7-ethinyl group in compound **10**, which enhances binding affinity compared to template **1**. The electronegative character of iodine in compound **8** is probably too weak to increase receptor binding. Also the large van der Waals radius of iodine may lower the binding affinity more than the methyl group of compound **9**, which has almost no effect.

The presence of a second aromatic ring system should be of considerable importance, as can be seen by the decrease of the binding data when replacing *p*-chlorophenyl by the sterically comparable cyclohexyl group (**11**). This dependence is not represented within the colored maps, because there is no mechanism within CoMFA to automatically recognize aromatic ring systems apart from their point charge distribution.

Application on a Test Set. For compounds **26**−**29** the CoMFA model was used to predict the D4 receptor binding affinities. Table 4 shows the experimental

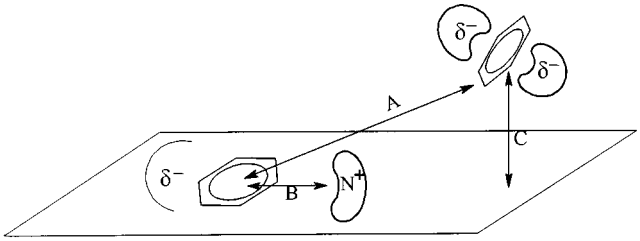

Figure 6. Pharmacophore model derived from the information of the CoMFA. A, B, and C represent distance ranges in Å (A: 7.5−8.5; B: 2.9−4.3; C: 2.5−3.5). Two planar π-systems are important: the first located above the plane is represented by a ring system (δ^- marks a negative area caused by a π-system or a nitrogen lone pair), while the second, which is positioned in the plane, stands for a conjugated moiety (generally a benzene ring) substituted with a bulky electronegative group. N^+ indicates a cationic nitrogen.

versus the calculated pK_i values. The overall performance of the model is satisfactory; no systematic deviation is noticeable. Apart from the trifluoromethyl derivative **28**, the deviations were smaller than 0.5 pK_i unit.

Pharmacophore Information. On the basis of the data obtained by the field analysis, we present a common pharmacophore, which summarizes important features necessary for effective D4 binding (Figure 6). All compounds should have a planar π-system, ideally substituted with a bulky, electronegative group. In a distance between 2.9 and 4.3 Å, a cationic nitrogen should be located near a plane defined by the π-moiety. A second π-system is placed about 2.5−3.5 Å above, with a distance of about 8 Å from the first π-moiety. In the case of clozapine, the situation is special, when the second electronegative system is provided by the lone pair of N_1.

Conclusion

We have shown that the experimentally obtained dopamine D4 receptor binding affinities of the arylmethylpiperazine derivatives **1**−**24** correlate well with the results of our theoretical CoMFA model. We succeeded to include the atypical antipsychotic drug clozapine (**25**) that shares only limited structural similarity with the other members of the dataset. This was achieved by applying a combined strategy for the very sensitive structural alignment of the antagonists. After a systematic conformational analysis of every ligand was performed, the actual overlay was done by optimizing a fit function consisting of steric and electrostatic properties within the translational and rotational space. It is important to mention that the overlay of the template **1** to clozapine was performed for every local minimum of **1** found by the semiempirical analysis, not only for the energetically most stable conformation. This is necessary, because it is well-known that receptors may bind ligands in a conformation which does not correspond to the thermodynamic minimum in the gas phase or even in solution.

Our final CoMFA model is able to predict the binding affinity of the 25 D4 antagonists to an accuracy of $q^2_{cv} = 0.784$. The increase due to the systematic rotation of the aligned molecules within the 1 Å lattice was only 0.045, indicating that the spatial dependence of the CoMFA method can be mostly compensated by decreasing the grid increment. It should be emphasized that one important limiting factor for the lattice refinement is the available computing time, which nevertheless allowed the application of a systematic orientational search procedure. The statistics of our CoMFA are sufficient to allow the prediction of reliable D4 binding affinities for new structures. Potential successful candidates should have at least a spatial extension comparable to that of **1**. The presence of two π-systems separated by a basic spacer like piperazinylmethyl should also be a prerequisite for effective binding. The overlay of the template compound **1** with clozapine showed that there is no need to directly match the basic nitrogens, which are often considered important pharmacophoric points. With this information in mind, the design, synthesis, and testing of new compounds are currently being investigated.

Acknowledgment. We thank Dr. Tim Clark (Computer Chemistry Center, University of Erlangen-Nuremberg) for a fruitful collaboration. This work was supported by the Fonds der Chemischen Industrie.

References

(1) *The Dopamine Receptors*; Neve, K. A., Neve, R. L., Eds.; Humana Press: Totowa, NJ, 1997.
(2) Sibley, D. R.; Monsma, F. J., Jr. Molecular Biology of Dopamine Receptors. *Trends Pharmacol. Sci.* **1992**, *13*, 61−69.
(3) Sokoloff, P.; Schwartz, J.-C. Novel Dopamine Receptors Half a Decade Later. *Trends Pharmacol. Sci.* **1995**, *16*, 270−275.
(4) Van Tol, H. H. M.; Bunzow, J. R.; Guan, H. C.; Sunahara, R. K.; Seeman, P.; Niznik, H. B.; Civelli, O. Cloning of the Gene for a human Dopamine D4 Receptor with high Affinity for the antipsychotic Clozapine. *Nature* **1991**, *350*, 610−614.
(5) Strange, P. G. Dopamine D4 Receptors: Curiouser and Curiouser. *Trends Pharmacol. Sci.* **1994**, *15*, 317−319. Liegeois, J.-F.; Eyrolles, L.; Bruhwyler, J.; Delarge, J. Dopamine D4 Receptors: A new Opportunity for Research on Schizophrenia. *Curr. Med. Chem.* **1998**, *5*, 77−100.
(6) Boyfield, I.; Brown, T. H.; Coldwell, M. C.; Cooper, D. G.; Hadley, M. S.; Hagan, J. J.; Healy, M. A.; Johns, A.; King, R. J.; Middlemiss, D. N.; Nash, D. J.; Riley, G. J.; Scott, E. E.; Smith, S. A.; Stemp, G. Design and Synthesis of 2-Naphthoate Esters as Selective Dopamine D_4 Antagonists. *J. Med. Chem.* **1996**, *39*, 1946−1948.
(7) Thurkauf, A.; Yuan, J.; Chen, X.; He, X. S.; Wasley, J. W. F.; Hutchison, A.; Woodruff, K. H.; Meade, R.; Hoffman, D. C.; Donovan, H.; Jones-Hertzog, D. K. 2-Phenyl-4(5)-[[4-(pyrimidin-2-yl)piperazin-1-yl]methyl]imidazole. A Highly Selective Antagonist at Cloned Human D_4 Receptors. *J. Med. Chem.* **1997**, *40*, 1−3.
(8) Rowley, M.; Collins, I.; Broughton, H. B.; Davey, W. B.; Baker, R.; Emms, F.; Marwood, R.; Patel, S.; Patel, S.; Ragan, C. I.; Freedman, S. B.; Ball, R.; Leeson, P. D. 4-Heterocyclylpiperidines as Selective High-Affinity Ligands at the Human Dopamine D4 Receptor. *J. Med. Chem.* **1997**, *40*, 2374−2385.
(9) Unangst, P. C.; Capiris, T.; Connor, D. T.; Doubleday, R.; Heffner, T. G.; MacKenzie, R. G.; Miller, S. R.; Pugsley, T. A.; Wise, L. D. (Aryloxy)alkylamines as Selective Human Dopamine D_4 Receptor Antagonists: Potential Antipsychotic Agents. *J. Med. Chem.* **1997**, *40*, 4026−4029.
(10) Glase, S. A.; Akunne, H. C.; Georgic, L. M.; Heffner, T. G.; MacKenzie, R. G.; Manley, P. J.; Pugsley, T. A.; Wise, L. D. Substituted [(4-Phenylpiperazinyl)methyl]benzamides: Selective Dopamine D_4 Agonists. *J. Med. Chem.* **1997**, *40*, 1771−1772.
(11) Wright, J. L.; Gregory, T. F.; Heffner, T. G.; MacKenzie, R. G.; Pugsley, T. A.; Vander Meulen, S.; Wise, L. D. Discovery of Selective Dopamine D4 Receptor Antagonists: 1-Aryloxy-3-(4-aryloxypiperidinyl)-2-propanols. *Bioorg. Med. Chem. Lett.* **1997**, *7*, 1377−1380.
(12) He, X. S.; Woodruff, K.; Brodbeck, R. A New Series of Selective Dopamine D_4 Ligands: 3-([4-Arylpiperazin-1-yl]alkylamino)-2H-1,4-benzoxazines. *Bioorg. Med. Chem. Lett.* **1997**, *7*, 2399−2402.
(13) Sanner, M. A.; Chappie, T. A.; Dunaiskis, A. R.; Fliri, A. F.; Desai, K. A.; Zorn, S. H.; Jackson, E. R.; Johnson, C. G.; Morrone, J. M.; Seymour, P. A.; Majchrzak, M. J.; Faraci, W. S.; Collins, J. L.; Duignan, D. B.; Di Prete, C. C.; Lee, J. S.; Trozzi, A. Synthesis, SAR and Pharmacology of CP-293,19: A Potent, Selective Dopamine D_4 Receptor Antagonist. *Bioorg. Med. Chem. Lett.* **1998**, *8*, 725−730.

(14) Bourrain, S.; Collins, I.; Neduvelil, J. G.; Rowley, M.; Leeson, P. D.; Patel, S.; Patel, S.; Emms, F.; Marwood, R.; Chapman, K. L.; Fletcher, A. E.; Showell, G. A. Substituted Pyrazoles as Novel Selective Ligands for the Human Dopamine D_4 Receptor. *Bioorg. Med. Chem.* **1998**, *6*, 1731−1743.

(15) Curtis, N. R.; Kulagowski, J. J.; Leeson, P. D.; Ridgill, M. P.; Emms, F.; Freedman, S. B.; Patel, S.; Patel, S. Synthesis and SAR of 2- and 3-Substituted 7-Azaindoles as Potential Dopamine D_4 Ligands. *Bioorg. Med. Chem. Lett.* **1999**, *9*, 585−588.

(16) Kesten, S. R.; Heffner, T. G.; Johnson, S. J.; Pugsley, T. A.; Wright, J. L.; Wise, L. D. Design, Synthesis, and Evaluation of Chromen-2-ones as Potent and Selective Human Dopamine D4 Antagonists. *J. Med. Chem.* **1999**, *42*, 3718−3725.

(17) Belliotti, T. R.; Wustrow, D. J.; Brink, W. A.; Zoski, K. T.; Shih, Y.-H.; Whetzel, S. Z.; Georgic, L. M.; Corbin, A. E.; Akunne, H. C.; Heffner, T. G.; Pugsley, T. A.; Wise, L. D. A Series of 6- and 7-Piperazinyl- and -Piperidinylmethylbenzoxazinones with Dopamine D4 Antagonist Activity: Discovery of a Potential Atypical Antipsychotic Agent. *J. Med. Chem.* **1999**, *42*, 5181−5187.

(18) Perrone, R.; Berardi, F.; Colabufo, N. A.; Leopoldo, M.; Tortorella, V. A Structure-Affinity Relationship Study on Derivatives of N-[2-[4-(4-Chlorophenyl)piperazin-1-yl]ethyl]-3-methoxybenzamide, a High-Affinity and Selective D_4 Receptor Ligand. *J. Med. Chem.* **2000**, *43*, 270−277.

(19) Arlt, M.; Böttcher, H.; Riethmüller, A.; Schneider, G.; Bartoszyk, G. D.; Greiner, H.; Seyfried, C. A. SAR of novel biarylmethylamine dopamine D4 receptor ligands. *Bioorg. Med. Chem. Lett.* **1998**, *8*, 2033.

(20) Kulagowski, J. J.; Broughton, H. B.; Curtis, N. R.; Mawer, I. M. Ridgill, M. P.; Baker, R.; Emms, F.; Freedman, S. B.; Marwood, R.; Patel, S.; Patel, S.; Ragan, C. I.; Leeson, P. D. 3-[[4-(4-Chlorophenyl)piperazin-1-yl]-methyl]-1*H*-pyrrolo[2,3-*b*]pyridine: An Antagonist with High Affinity and Selectivity for the Human Dopamine D4 Receptor. *J. Med. Chem.* **1996**, *39*, 1941−1942.

(21) Löber, S.; Hübner, H.; Gmeiner, P. Azaindole Derivatives with High Affinity for the Dopamine D4 Receptor: Synthesis, Ligand Binding Studies, and Comparison of Molecular Electrostatic Potential Maps. *Bioorg. Med. Chem. Lett.* **1999**, *9*, 97−102.

(22) Haubmann, C.; Hübner, H.; Gmeiner, P. 2,2-Dicyanovinyl as a Nonaromatic Aryl Bioisostere: Synthesis, Binding Experiments and SAR Studies of Highly Selective Dopamine D4 Receptor Ligands. *Bioorg. Med. Chem. Lett.* **1999**, *9*, 1969−1972.

(23) Hübner, H.; Haubmann, C.; Gmeiner, P. Conjugated Enynes as Nonaromatic Catechol Bioisosteres: Synthesis, Binding Experiments, and Computational Studies of Novel Dopamine Receptor Agonists Recognizing Preferentially the D_3 Subtype. *J. Med. Chem.* **2000**, *43*, 756−762.

(24) Einsiedel, J.; Thomas, C.; Hübner, H.; Utz, W.; Gmeiner, P. Phenyloxazoles and Phenylthiazoles as Benzamide Bioisosteres: Synthesis and Dopamine Receptor Binding Profiles. *Bioorg. Med. Chem. Lett.* **2000**, *10*, 2041−2044.

(25) Cramer, R. D., III; Depriest, S.; Patterson, D.; Hecht, P. The developing practice of comparative molecular field analysis. In *3D QSAR in Drug Design − Theory, Methods, and Applications*; Kubinyi, H., Ed.; ESCOM: Leiden, 1993; pp 443−485.

(26) Homan, E. J.; Tulp, M. T. M.; Nilsson, J. E.; Wikstrom, H. V.; Grol, C. J. C5-Substituted derivatives of 5-OMe-BPAT: synthesis and interactions with dopamine D2 and serotonin 5-HT1A receptors. *Bioorg. Med. Chem.* **1999**, *7*, 2541−2548.

(27) McGaughey, G. B.; Mewshaw, R. E. Application of comparative molecular field analysis to dopamine D2 partial agonists. *Bioorg. Med. Chem.* **1999**, *7*, 2453−2456.

(28) Wilcox, R. E.; Tseng, T.; Brusniak, M.-Y. K.; Ginsburg, B.; Pearlman, R. S.; Teeter, M.; DuRand, C.; Starr, S.; Neve, K. A. CoMFA-Based Prediction of Agonist Affinities at Recombinant D1 vs D2 Dopamine Receptors. *J. Med. Chem.* **1998**, *41*, 4385−4399.

(29) Nilsson, J.; Wikstroem, H.; Smilde, A.; Glase, S.; Pugsley, T.; Cruciani, G.; Pastor, M.; Clementi, S. GRID/GOLPE 3D Quantitative Structure−Activity Relationship Study on a Set of Benzamides and Naphthamides, with Affinity for the Dopamine D3 Receptor Subtype. *J. Med. Chem.* **1997**, *40*, 833−840.

(30) Asghari, V.; Sanyal, S.; Buchwaldt, S.; Paterson, A.; Jovanovic, V.; Van Tol, H. H. M. Modulation of intracellular cyclic AMP levels by different human Dopamine D4 Receptor variants. *J. Neurochem.* **1995**, *65*, 1157−1165.

(31) Löber, S. Subtypselektive Dopaminrezeptor-Liganden mit Diazol-Partialstruktur. Ph.D. Thesis, Erlangen, 2000.

(32) Seeman, P. Dopamine Receptor Sequences: Therapeutic Levels of Neuroleptics Occupy D_2 Receptors, Clozapine occupies D_4. *Neuropsychopharmacology* **1992**, *7*, 261−284.

(33) Schmutz, J. Neuroleptic Piperazinyl-dibenzo-azepines. *Arzneim.-Forsch. (Drug Res.)* **1975**, *25*, 712−720.

(34) Chakrabarti, J. K.; Hotten, T. M.; Morgan, S. E.; Pullar, I. A.; Rackham, D. M.; Risius, F. C.; Wedley, S.; Chaney, M. O.; Jones, N. D. Effects of Conformationally Restricted 4-Piperazinyl-10*H*-thienobenzodiazepine Neuroleptics on Central Dopaminergic and Cholinergic Systems. *J. Med. Chem.* **1982**, *25*, 1133−1140.

(35) Dewar, M. J. S.; Zoebisch, E. G.; Healey, E. F.; Stewart, J. J. P. AM1: A New General Purpose Quantum Mechanical Model. *J. Am. Chem. Soc.* **1985**, *107*, 3902−3909.

(36) Frisch, M. J.; Trucks, G. W.; Schlegel, H. B.; Gill, P. M. W.; Johnson, B. G.; Robb, M. A.; Cheeseman, J. R.; Keith, T.; Petersson, G. A.; Montgomery, J. A.; Raghavachari, K.; Al-Laham, M. A.; Zakrzewski, V. G.; Ortiz, J. V.; Foresman, J. B.; Cioslowski, J.; Stefanov, B. B.; Nanayakkara, A.; Challacombe, M.; Peng, C. Y.; Ayala, P. Y.; Chen, W.; Wong, M. W.; Andres, J. L.; Replogle, E. S.; Gomperts, R.; Martin, R. L.; Fox, D. J.; Binkley, J. S.; Defrees, D. J.; Baker, J.; Stewart, J. P.; Head-Gordon, M.; Gonzalez, C.; Pople, J. A. *Gaussian 94*, revision E.2; Gaussian, Inc.: Pittsburgh, PA, 1995.

(37) Klamt, A.; Schüümann, G. COSMO: A New Approach to Dielectric Screening in Solvents with Explicit Expressions for the Screening Energy and its Gradient. *J. Chem. Soc., Perkin Trans. 2* **1993**, 799−805.

(38) Liotard, D. A.; Hawkins, G. D.; Lynch, G. C.; Cramer, C. J.; Truhlar D. G. Improved methods for semiempirical solvation models. *J. Comput. Chem.* **1995**, *16*, 422−440.

(39) Hawkins, G. D.; Lynch, G. C.; Giesen, D. J.; Rossi, I.; Storer, J. W.; Truhlar, D. G.; Liotard, D. A.; Cramer, C. J.; Truhlar, D. G. Quantum Chemistry Program Exchange Program 606.

(40) *Exploring Chemistry with Electronic Structure Methods*; Foresman, J. B., Frisch, A. E., Eds.; Gaussian, Inc.: Pittsburgh, PA, 1996; p 168.

(41) Klebe, G.; Abraham, U. On the Prediction of Binding Properies of Drug Molecules by Comparitative Molecular Field Analysis. *J. Med. Chem.* **1993**, *36*, 70−80.

(42) Mattos, C.; Ringe, D. Multiple Binding Modes. In *3D QSAR in Drug Design;* Kubinyi, H., Ed.; ESCOM: Leiden, 1993; pp 226−254.

(43) Clark, T.; Alex, A.; Beck, B.; Chandrasekar, J.; Gedeck, P.; Horn, A.; Huttern, M.; Martin, B.; Rauhut, G.; Sauer, W.; Schindler, T.; Steinke, T. *Program Package VAMP 7.0;* Oxford Molecular Group Plc.: Oxford, 1998.

(44) *ASP V 3.22*; Oxford Molecular Ltd., The Medawar Centre, Oxford Science Park, Sandford-on-Thames, Oxford OX4 4GA, U.K.

(45) *TSAR V 3.2*; Oxford Molecular Ltd., The Medawar Centre, Oxford Science Park, Sandford-on-Thames, Oxford OX4 4GA, U.K.

(46) Beck, B.; Glen, R. C.; Clark, T. A Detailed Study of VESPA Electrostatic Potential-Derived Atomic Charges. *J. Mol. Model.* **1995**, *1*, 176−187.

(47) Carbo, R.; Leyda, L.; Arnau M. How similar is a molecule to another? An electron density measure of similarity between two molecular structures. *Int. J. Quantum Chem.* **1980**, *17*, 1185−1189.

(48) *SYBYL 6.6*; Tripos Inc., 1699 South Hanley Rd., St. Louis, MO 63144.

(49) Clark, M.; Cramer, R. D., III; Van Opdenbosch, N. Validation of the general purpose Tripos 5.2 force field. *J. Comput. Chem.* **1989**, *10*, 982−1012.

(50) Gasteiger, J.; Marsili, M. Iterative partial equalization of orbital electronegativity: a rapid access to atomic charges. *Tetrahedron* **1980**, *36*, 3219−3222.

(51) Dunn, W. J.; Wold, S.; Edlund, V.; Helberg, S. Multivariate structure−activity relationships between data from a battery of biological tests and an ensemble of structure descriptors: the PLS method. *Quantum Struct.-Act. Relat.* **1984**, *3*, 131−137.

(52) Tropsha, A.; Cho, S. J. Cross-Validated R^2 Guided Region Selection for CoMFA Studies. In *3D QSAR in Drug Design;* Kubinyi, H., Ed.; ESCOM: Leiden, 1998; Vol. 3, pp 57−69.

(53) Wang, R.; Gao, Y.; Lai, L. All-Orientation Search and All-Placement Search in Comparative Molecular Field Analysis. *J. Mol. Model.* **1998**, *4*, 276−283.

(54) Böhm, M.; Stürzebecher, J.; Klebe, G. Three-Dimensional Quantitative Structure−Activity Relationship Analyses Using Comparative Molecular Field Analysis and Comparative Molecular Similarity Indices Analysis To Elucidate Selectivity Differences of Inhibitors Binding to Trypsin, Thrombin, and Factor Xa. *J. Med. Chem.* **1999**, *42*, 458−477.

(55) Klebe, G.; Abraham, U.; Mietzner, T. Molecular Similarity Indices in a Comparative Analysis (CoMSIA) of Drug Molecules to Correlate and Predict Their Biological Activity. *J. Med. Chem.* **1994**, *37*, 4130−4146.

JM001055E